Journal of
Mechanical
Science and
Technology

Journal of Mechanical Science and Technology 21 (2007) 525~535

Numerical Simulation of Auto-Regulation and Collateral Circulation in the Human Brain

Changsung Sean Kim*

Principal Research Engineer, Samsung Electro-Mechanics Co. Ltd.
Coporate R&D Institute, Suwon 443-743, Korea.

(Manuscript Received May 24, 2006; Revised July 27, 2006; Accepted January 10, 2007)

Abstract

A novel approach using computational fluid dynamics (CFD) and magnetic resonance image (MRI) is applied to model the auto-regulation and blood flow in the human brain. To provide a basic understanding of the auto-regulation mechanism in the brain, an anatomical Circle of Willis configuration is reconstructed from subject-specific magnetic resonance images using image segmentation methods and grid generation techniques. The three-dimensional unsteady incompressible Navier-Stokes equations are solved iteratively using the pseudocompressibility method and dual time stepping method. For the efficient simulation of three-dimensional time-dependent flows, parallel computations based on a domain decomposition method are performed. A simple auto-regulation algorithm is presented to model the dynamic peripheral resistance due to arteriolar contraction and dilatation. The present numerical methods are then used to simulate the auto-regulation of blood flow in the realistic Circle of Willis model with geometrical variants. The computed results show the correlation between abnormal vascular structures and the auto-regulation mechanism in the cerebral circulation.

Keywords: Auto-regulation, Collateral circulation, Human brain, Computational fluid dynamics (CFD), Magnetic resonance image (MRI), Circle of willis, Cerebral circulation

1. Introduction

The brain has a unique vascular structure, so-called the Circle of Willis, a network of arteries able to provide collateral blood flow to both hemispheres. There are two paired arteries that supply blood to the brain. One pair is the left and right internal carotid arteries (ICA) and the other is the left and right vertebral arteries. The vertebral arteries are distally combined into the basilar artery that ends by dividing into two posterior cerebral arteries (PCA). The left and right ICA and the basilar artery are connected to the Circle formed by a single anterior communicating artery (ACoA) and the paired anterior cerebral artery (ACA), posterior communicating (PCoA) and posterior cerebral (PCA) arteries. A three-dimensional model of the idealized Circle of Willis is shown in Fig. 1. The Circle of Willis sits on the base of the brain and its main function is to distribute blood evenly throughout the brain. When the flow into the cerebral tree is asymmetric, that is, if one of the major afferent arteries becomes stenosed or occluded, blood flows through the Circle so as to maintain sufficient blood to all of the cerebral tissue, termed collateral circulation.

More importantly, in addition to collateral circulation, the arterial tree can vary its vessel radius dynamically to accommodate temporal changes of the

*Corresponding author. Tel.: +82 31 300 7847, Fax.: +82 31 210 6286
E-mail address: csean.kim@samsung.com

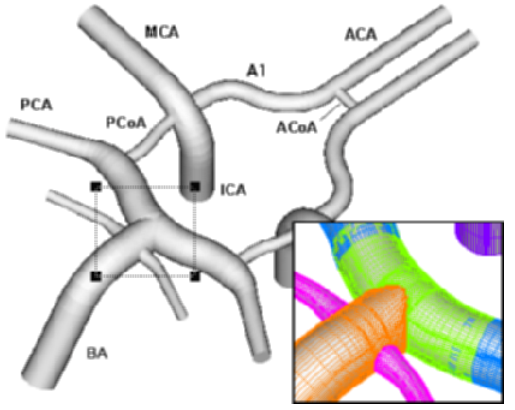

ACA: Anterior Cerebral Artery, ACoA: Anterior Communicating Artery,
BA: Basilar Artery, ICA: Internal Carotid Artery, MCA: Middle Cerebral Artery,
PCA: Posterior Cerebral Artery, PCoA: Posterior Communicating Artery.
Fig. 1. A three-dimensional model of an idealized Circle of Willis configuration [Kim et. al., 2006].

perfusion pressure (most notably done by the arterioles) and thus maintain the required blood flow. This is termed auto-regulation and is an active method for delivering the correct blood mass flux to the brain. Figure 2 shows an example of the auto-regulatory response after a sudden drop in perfusion pressure. Flow rate begins to increase back toward control by decreasing the vascular resistance. Cerebral arteries dilate or contract in order to adjust the resistance depending on relatively abrupt changes in mean arterial pressure. This dilation/contraction is accomplished through the expansion/contraction of the smooth muscle cells surrounding the arterial lumen. The brain auto-regulates blood flow within a certain range of perfusion pressure as shown in Fig. 3. There is a lower limit of perfusion pressure below which cerebral arteries are maximally vaso-dilated and blood flow decreases passively with further reduction in perfusion pressure. Also, there is an upper limit to the auto-regulation range which is seldom reached physiologically.

It is clear that human experiments would be very difficult if not impossible to perform in vivo. However numerical models have become available which can model the cerebro-vascular tree and the auto-regulation. Kufahl and Clark (1985) developed a one-dimensional finite difference model with distensible

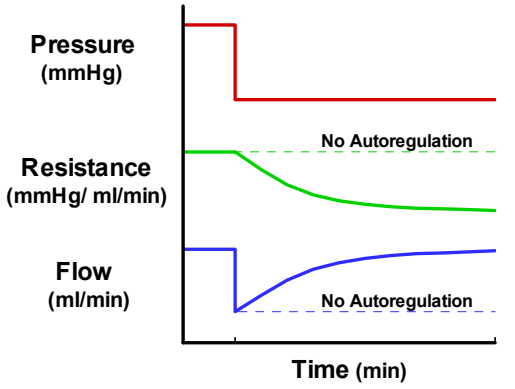

Fig. 2. Auto-regulatory response after sudden drop in perfusion pressure.

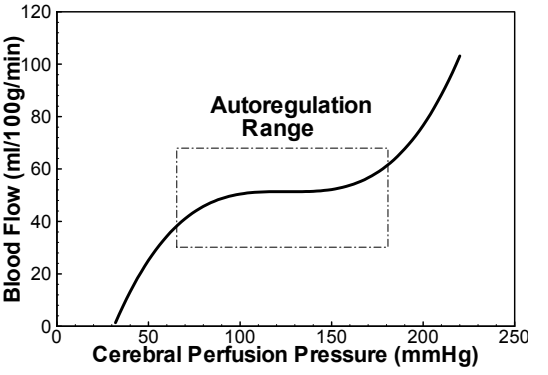

Fig. 3. Cerebral auto-regulation curve of blood flow vs. perfusion pressure.

vessels for both steady and pulsatile flows in the Circle of Willis. Hillen et al. (1988) has provided one-dimensional models of the Circle of Willis to describe the relationship between the flow rate, vascular resistance and pressure using Hagen-Poiseuille formula. They concluded that the efferent fluxes were dependent on the distribution of the efferent resistance, and that there was a relationship between the mass flux and the anatomical structure of the Circle of Willis. Ferrandez and David (2000) and Ferrandez et al. (2002) have shown that both arterial geometry and the proper functioning of the auto-regulation mechanism are crucial in determining not only the correct amount of blood supply to the brain but also in characterising possible "unstable" geometric variants of the Circle of Willis. Olufsen et al. (2002) used a lumped parameter model to explain dynamics of cerebral blood flow response to hypotension during posture change.

For the purpose of numerical modeling, minor arteries such as arterioles and capillaries need to be truncated to perform the numerical simulation due to computational expense. At the truncated position where flow information is not available, equivalent outflow boundary conditions are necessary. Lumped models utilizing the analogy of arterial networks to electric circuits have been used to provide the adequate boundary conditions for three-dimensional computations (e.g., Quarteroni et al., 2000; Formaggia et al., 2002). A vascular bed model was adopted to impose pressure boundary conditions at outflow boundaries (Cebral et al., 2000). Also Ferrandez et al. (2002) have defined a novel boundary condition using a control theory in order to simulate the peripheral resistance of the cerebro-vascular tree and its auto-regulation function.

Specific shapes and connections of the brain arterial tree vary in the human population (Alpers et al., 1959). Three-dimensional reconstruction techniques have been used to obtain the subject-specific vasculature from magnetic resonance imaging (MRI), magnetic resonance angiogram (MRA), and computed tomography (CT) (e.g., Taylor et al., 1999; Cebral et al., 2000; Quarteroni et al., 2000; Steinman et al., 2002; Zhao et al., 2002). Computational simulations coupled with those medical imaging techniques can provide the physicians with patient-specific information to predict the outcome of surgical procedures. Besides, flow variables that are difficult to measure in vivo can be calculated using real geometries. Considering the geometric variations, computational approach will offer an economical alternative to experiments on in vitro models.

Recently, there have been some numerical studies on computational modeling of the patient-specific vascular structure and auto-regulation mechanism in the human brain. Cebral et al. (2000) simulated the blood flows in patient-specific cases taken from MRA images as a planning tool for neuro-surgical and interventional procedures. Kim et al. (2006) provided numerical models to simulate the collateral circulation in a subject-specific Circle of Willis under altered gravity conditions. In the present study, a three-dimensional model of the anatomical Circle of Willis is developed and several examples of the auto-regulation mechanism are simulated to demonstrate the relationship between geometrical abnormalities and the auto-regulation performance in the cerebral circulation.

2. Computational approach

2.1 Blood flow model

The blood flow is modeled applying the three-dimensional, unsteady, incompressible Navier-Stokes equations. The system of equations can be written in tensor notation form as:

$$\frac{\partial u_k}{\partial x_k} = 0 \tag{1}$$

$$\frac{\partial u_i}{\partial t} + \frac{\partial}{\partial x_j}\left(u_j u_i\right) = -\frac{\partial p}{\partial x_i} + \frac{\partial \tau_{ij}}{\partial x_j} + g_i \tag{2}$$

The shear stress tensor, τ_{ij} is defined as:

$$\tau_{ij} = 2\mu(\dot{\gamma})S_{ij} \tag{3}$$

where $\mu(\dot{\gamma})$ is the apparent viscosity, S_{ij} is the mean strain-rate tensor, and $\dot{\gamma}$ is the shear rate defined as a function of the second invariant of S_{ij} in three-dimensional problems:

$$S_{ij} = \frac{1}{2}\left(\frac{\partial u_i}{\partial x_j} + \frac{\partial u_j}{\partial x_i}\right) \tag{4}$$

$$\dot{\gamma} = 2\sqrt{\mathrm{II}_S} = \sqrt{2\left(S_{ij}S_{ij} - {S_{kk}}^2\right)} \tag{5}$$

In the present study, an MPI parallel version of the IFANS3D code (Kim et al., 2001) was used to solve the incompressible Naiver-Stokes equations in three-dimensional generalized coordinates for both steady-state and time varying flow. The equations are formulated into a hyperbolic set of partial differential equations using the pseudocompressibility method. The convective terms are differenced using an upwind biased flux-difference splitting. The equations are solved using an implicit line-relaxation scheme. More details about these numerical schemes are found elsewhere (Rogers, et al., 1991; Kiris et al., 1997; Kwak et al., 2005).

The complex fluid behavior of blood was approximated using a Carreu-Yasuda model (Gijsen et al., 1999; Kim et al., 2006). This model derived in

Eq. (6) describes the shear thinning behavior of blood flows with asymptotic apparent viscosities, μ_0 and μ_∞, at zero and infinite shear rates, respectively.

$$\mu(\dot{\gamma}) = \mu_\infty + (\mu_0 - \mu_\infty)\left[1 + (\lambda\dot{\gamma})^a\right]^{\frac{n-1}{a}} \tag{6}$$

where the constitutive parameters of the human blood are given as

$$\mu_\infty = 0.00348 Pa\cdot s,\ \mu_0 = 0.1518 Pa\cdot s,\\ \lambda = 40.0 s,\ a = 2.0,\ n = 0.356 \tag{7}$$

2.2 Vascular bed model

To make the problem computationally manageable, minor arteries such as arterioles and capillaries need to be truncated. An equivalent outflow boundary condition should be imposed at the truncated position. There is an analogy between the arterial network and the electric circuit as shown in Fig. 4. Flow resistance corresponds to electric resistance, flow rate to electric current, and pressure drop to electric voltage. The truncated artery is assumed to divide into N branches of the same size, for instance, N equals two for bifurcation and three for trifurcation. Under this assumption, the outflow boundary condition, especially for pressure, has been approximated by utilizing the electric circuit analogy and the Poiseuille's theorem (Nichols and O'Rourke, 1998; Cebral et al., 2000).

The pressure drop in each branch can be expressed with the Poiseuille's formula as

$$\Delta p_k = \frac{8\pi\mu L_k}{A_k^2}\dot{Q}_k = \mathrm{R}_k\dot{Q}_k,\quad \dot{Q}_{k+1} = \frac{1}{N}\dot{Q}_k \tag{8}$$

$$\Delta p_{k+1} = \mathrm{R}_{k+1}\dot{Q}_{k+1} = \frac{1}{N}\left(\frac{\mathrm{R}_{k+1}}{\mathrm{R}_k}\right)\Delta p_k = f\,\Delta p_k,\quad f = \frac{1}{N}\left(\frac{\mathrm{R}_{k+1}}{\mathrm{R}_k}\right) \tag{9}$$

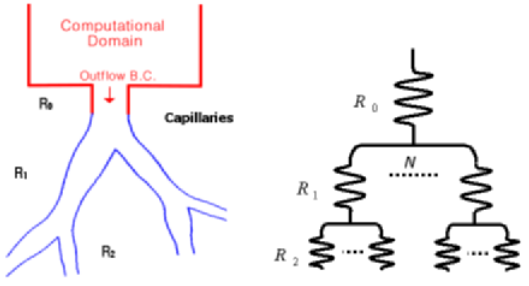

Fig. 4. Analogy of arterial network to electric circuit.

where $\dot{Q}$ is mass flow rate, p is pressure, and R is flow resistance. At the kth branch, its mass flow rate is N times of flow rate through the (k-1)st branch. Assuming that the flow resistance ratio f is constant and less than one, the total pressure difference between the outflow boundary p_0 and the capillary bed p_c is derived from the geometrical series form as

$$\Delta p_{total} = p_0 - p_c = \sum_{k=0}^{\infty}\Delta p_k = \frac{1}{1-f}\Delta p_0 = \frac{8\pi\mu L_0}{(1-f)A_0^2}\dot{Q}_0 \tag{10}$$

where subscript 0 represents the outflow boundary of the computational domain, A and L are sectional area and length of the vessel, respectively. The flow resistance ratio f is generally unknown and thus should be determined properly to avoid an unrealistic pressure drop at the capillary bed. The optimal value of f can be determined from the arteriolar auto-regulation model in the next section.

2.3 Arteriolar auto-regulation model

The arteriolar bed varies its flow resistance dynamically by dilating or constricting in order to maintain the constant blood flow within a certain range of the perfusion pressure. In order to model this feedback mechanism in the arteriolar bed, the arteriolar auto-regulation (AAR) algorithm is presented based on the vascular bed modeling in Eq.(10). Using the flow rate at the nth time step, the outflow pressure at the next time step is updated with the flow resistance ratio f until the flow rate satisfies the reference flow rate, $\dot{Q}_{ref}$.

$$p_0^{n+1} = p_c + \frac{8\pi\mu L_0}{(1-f^{n+1})A_0^2}\dot{Q}_0^n \tag{11}$$
$$f^{n+1} = 1 - 0.5/a^{n+1}$$
$$a^{n+1} = a^n + k_t\frac{(\dot{Q}_0^n - \dot{Q}_{ref})}{\dot{Q}_{ref}}$$
$$k_t = \alpha\Delta t/T$$

where α is a recovery coefficient that produces a reasonable autoregulatory response, and Δt and T are physical time step and period of the heart beat, respectively. Simultaneously, the velocity components at the outflow boundary are extrapolated from the interior domain.

2.4 Three-dimensional reconstruction

A three-dimensional CoW geometry was reconstructed from subject-specific magnetic resonance (MR) angiography (MRA) using an image segmentation technique as illustrated in Fig. 5. The raw MR images were converted to the RGB graphic file format for efficient numerical treatments. After extracting the segments of interest by filtering the voxels with intensities below a certain threshold, a segment outlining algorithm was used to display the extracted objects on each cross-sectional layer with very little computer memory. A commercial grid generation software (Gridgen) was used to create a three-dimensional surface database by stacking the two-dimensional transverse outlines. A certain degree of human intervention was required for the complete connectivity between surface domains. Consequently, a multi-block grid system with thirty-one domains was generated for this geometry as shown in Fig. 6.

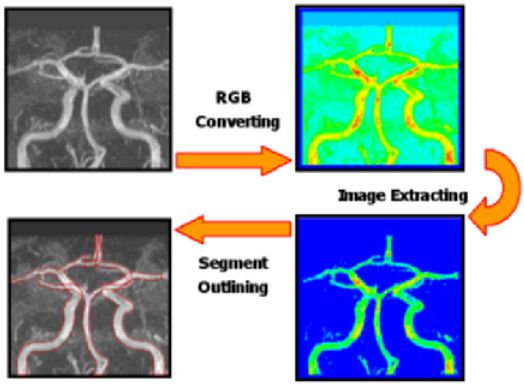

Fig. 5. Image segmentation from a magnetic resonance image for a subject-specific Circle of Willis [Kim et. al., 2006].

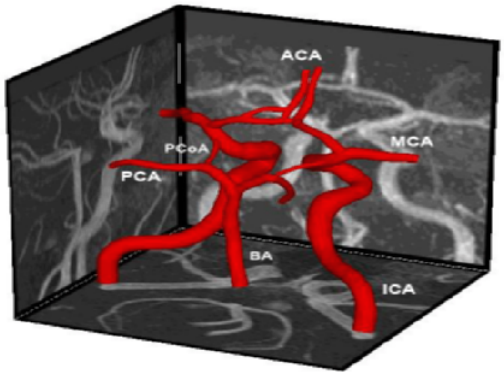

Fig. 6. Three-dimensional reconstruction of an anatomical Circle of Willis configuration [Kim et. al., 2006].

3. Results and Discussion

3.1 Idealized Circle of Willis model

To provide a preliminary understanding of the auto-regulation mechanism in the brain, an idealized Circle of Willis model was designed based on the anatomical measurements (Alpers et al., 1959; Gray, 1918) with minor arteries truncated. A multi-block grid system with ten domains for this idealized configuration was already shown in Fig. 1. Grid variables were non-dimensionalized by the ICA diameter of 5.6 mm. The left and right ICA and the basilar artery were assumed to have the same inflow rate of 3.5 ml/s for this configuration. Inflows were assumed to be fully developed. The AAR algorithm was used to impose dynamic outflow boundary conditions as well as to simulate the auto-regulation mechanism in the brain. The Reynolds number based on the ICA diameter is 240.

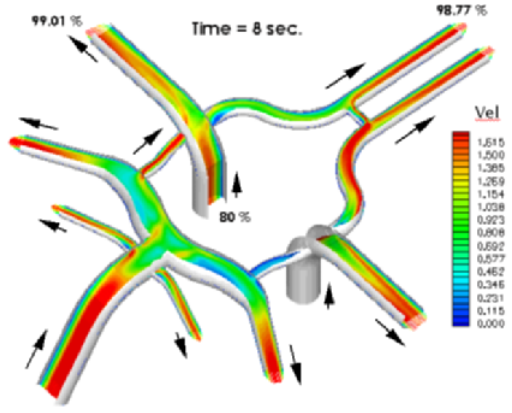

Fig. 7. Collateral circulation with the left internal carotid artery 20 % stenosed under auto-regulation. (Magnitude of normalized velocity in color contour.)

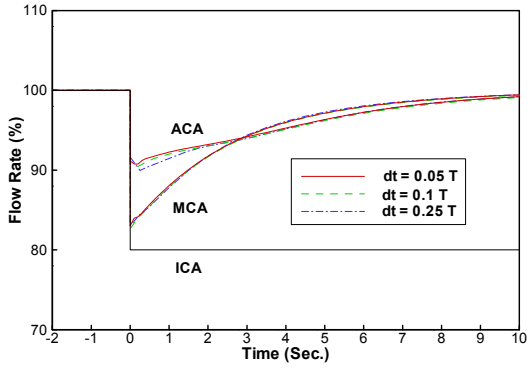

Fig. 8. Percent changes of flow rate in left middle and anterior cerebral arteries under auto-regulation.

When one of the main arteries in the brain is stenosed or even missing, the distal smaller arteries can receive blood from the other arteries through the Circle of Willis. To simulate this interesting mechanism of collateral circulation under auto-regulation, the left ICA is presumed 20 percent stenosed. This means that only 80 percent of the normal supply of blood is delivered to the Circle through the left ICA as indicated in Fig. 7. Unlike the balanced configuration case, the mass flux through the posterior communicating arteries (PCoA) and anterior communicating artery (ACoA) is considerably increased to compensate for the deficiency in the left middle cerebral artery (MCA). On the other hand, the mass flux through the proximal part (A1 segment) of the left anterior cerebral artery (ACA) is decreased by 26 percent in order to distribute the blood as evenly as possible. Figure 8 shows the time-dependent auto-regulatory process using the AAR algorithm. The ratio of the reference flow rates, $\dot{Q}_{ref}$ in Eq. (11) between MCA, PCA, and ACA was given as 6:4:3 in order to maintain a negligible mass flux through PCoA. This AAR algorithm was found to be robust and consistent for a wide range of physical time steps (dt = 0.05T to 0.25T). The optimal value for α was given by 8.0 for the adequate feedback time. Within about 10 seconds after the sudden stenosis in the left ICA, the left MCA and ACA have regained their initial (or reference) flow rates. The present simulation shows a good example of collateral circulation in the brain under auto-regulation.

3.2 Anatomical circle of willis model

In order to simulate the auto-regulating blood flow in a realistic configuration, an anatomical Circle of Willis model was reconstructed from subject-specific MRA images as already shown in Fig. 6. Spatial coordinates were normalized by the left ICA diameter of 5.6 mm. Total grid size was about 1.2 million node points. Considering the cross-sectional area, inflow rates through the ICA and the basilar artery were given as 3.5 and 2.1 ml/s, respectively. Pressure outflow boundary conditions were determined using Eq. (11) and the velocity components were extrapolated from the interior domain. The Reynolds number based on the left ICA diameter is 240.

As simulated in the previous example with the idealized model, the left ICA is assumed to be 20 percent stenosed and thus only 80 percent of the blood is delivered through the left ICA. The AAR algorithm was used to simulate the time-dependent response of auto-regulation. The ratio of the reference flow rates, $\dot{Q}_{ref}$ in Eq. (11) between MCA, PCA, and ACA was given as 7:3:3 in order to maintain a negligible mass flux through the PCoA. For efficient simulation, time step was given as dt = 0.1T and α = 8.0 for the adequate response.

3.3 Original configuration

The original configuration of the subject-specific Circle of Willis was tested to simulate time-dependent changes in flow rate through efferent arteries under auto-regulation. Figure 9 (a) shows the distribution and direction of flow in the Circle of Willis model before a sudden stenosis in the left ICA. As mentioned above, it was observed that both left and right PCoA as well as ACoA have very low mass flux under this normal condition. Figures 9 (b)-(d) show temporal flow distribution in the Circle of Willis model under auto-regulation. Initially, the left MCA has a 16 percent loss in mass flux whereas the left ACA has only a 5 percent loss as shown in Fig. 9 (b). Compared with the normal case in Fig. 9 (a), mass flux through the left PCoA and ACoA starts to increase considerably in order to supply more flux to the left MCA and ACA, respectively. However, the mass flux through the right PCoA is still very low. After 7 seconds, the left MCA recovers 99 percent of the initial amount as shown in Figure 9 (d). The time-dependent flow rates of the left MCA and ACA after a sudden stenosis in the left ICA are plotted in Fig. 10. Within approximately 10 seconds, the left MCA and ACA have regained their initial (or reference) flow rates.

3.4 No auto-regulation

For the same event of 20 percent stenosis in the left ICA, a critical situation where cerebral auto-regulation fails was also considered to simulate the collateral circulation without auto-regulation. With malfunctioning of auto-regulation mechanism, cerebral arterioles can neither dilate nor contract dynamically to accommodate temporal changes of the perfusion pressure. Consequently, the peripheral resistance maintains constant even though a sudden

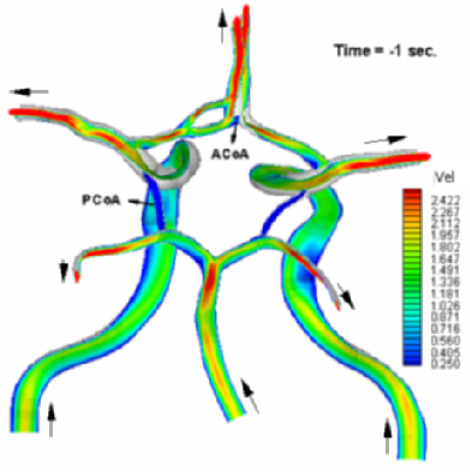

(a) Before the sudden stenosis in the left ICA

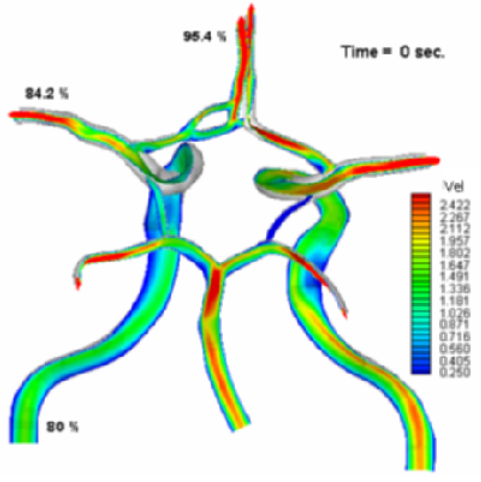

(b) After the sudden stenosis in the left ICA: Time = 0 sec

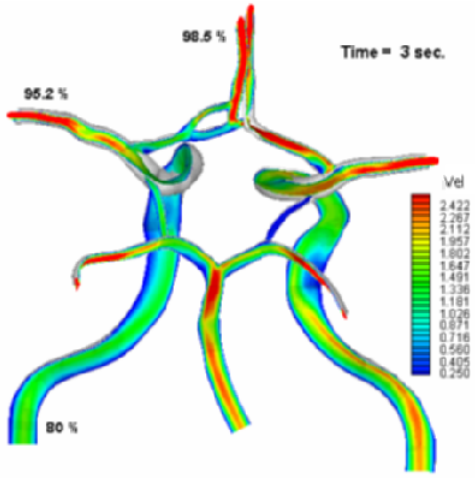

(c) Time = 3 sec

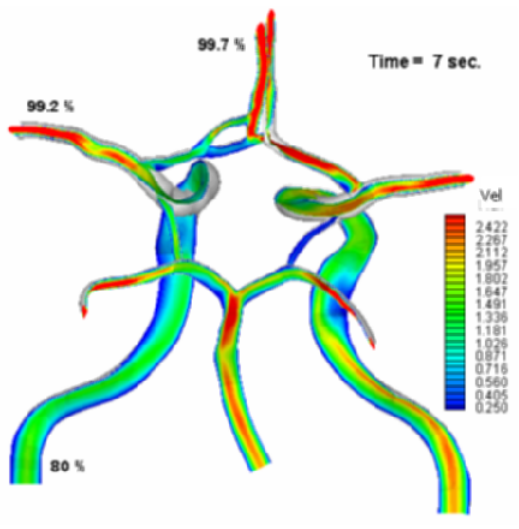

(d) Time = 7 sec

Fig. 9. Collateral circulation in the Circle of Willis with a sudden stenosis in the left ICA. (Magnitude of normalized velocity in color contour.)

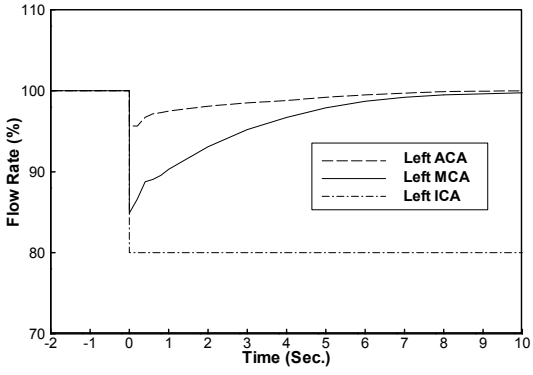

Fig. 10. Percent changes of flow rate in left middle and anterior cerebral arteries under auto-regulation.

drop in mass flux happens in afferent arteries. Fig. 11 (i.e., a snapshot after 7 seconds) makes little difference in the flow distribution from Fig. 9 (b). It is noticed that, without auto-regulation mechanism, the stenosis in the left ICA will cause a severe ischemic damage to the brain tissue in the left hemisphere. Fig. 12 indicates that mass fluxes have increased only 1.5 percent and 0.3 percent in the left MCA and ACA, respectively. Both the arteries fail to recover their initial mass fluxes. It is evident that proper functioning of auto-regulation mechanism is crucial to the normal cerebral circulation.

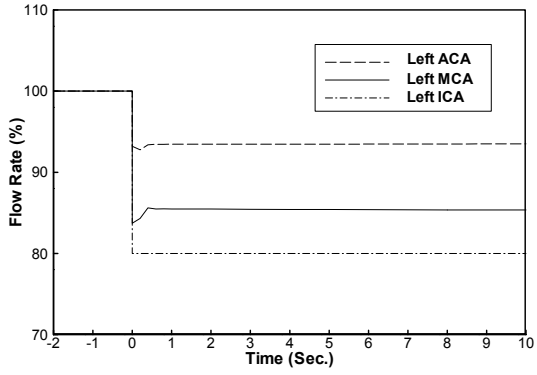

Fig. 12. Percent changes of flow rates without auto-regulation.

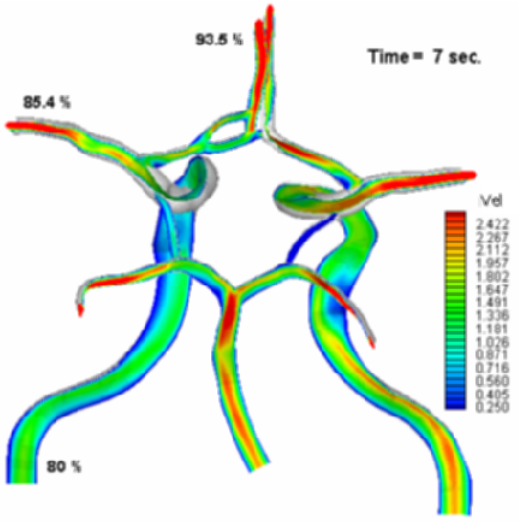

Fig. 11. Collateral circulation without auto-regulation mechanism.

3.5 Missing left PCoA

Under normal condition, mass fluxes through both PCoA were negligible as already seen in Fig. 9 (a). In the case of a sudden stenosis in the left ICA, however, mass flux through the left PCoA was considerably increased as shown in Fig. 9(d). The PCoA play an important role in collateral circulation under abnormal conditions. Thus, the effect of missing left PCoA on the auto-regulating flow in the Circle of Willis was simulated (Fig. 13). This configuration of interest can be representative of a string-like vessel or arterial occlusion of the left PCoA.

The initial drop in mass flux was 18 percent for the left MCA and 5.6 percent for the left ACA as shown in Fig. 13 (a). After 10 seconds later, as shown in Fig. 13 (b), the fluxes through ACoA and the right A1

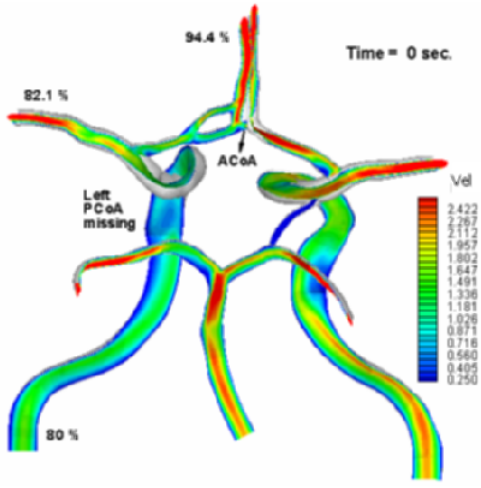

(a) Initial flow distribution: Time = 0 sec

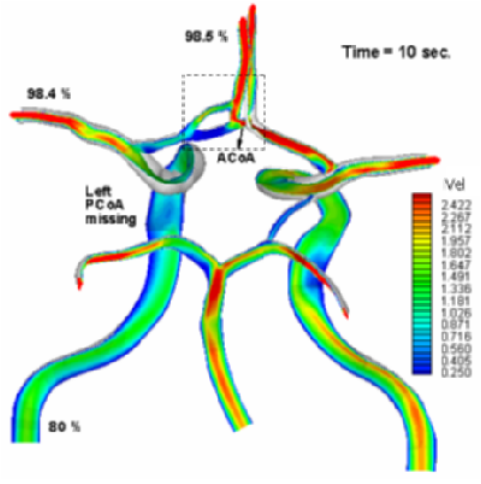

(b) Time = 10 sec

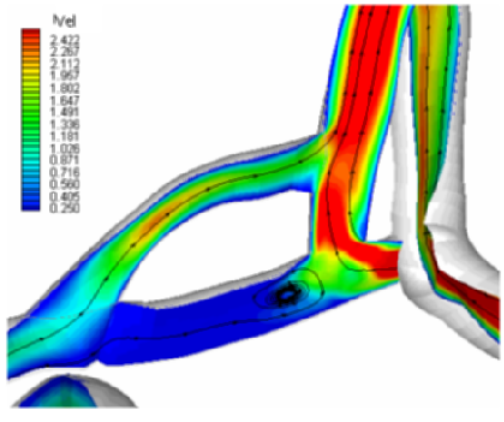

(c) Zoomed view: Time = 10 sec

Fig. 13. Flow redistribution in case of missing the left PCoA.

segment are remarkably increased to deliver more blood to the left ACA. There is a slight increase of mass flux through the right PCoA. The flow distribution around ACoA is zoomed in Fig. 13 (c). The lower A1 segment on the left has a very low mass flux and secondary flow pattern due to the adverse pressure gradient. This three-dimensional model can capture particular flow physics not treatable in one- and two-dimensional models. Figure 14 shows that both mass fluxes in the left MCA and ACA have regained about 98 percent after 10 seconds. It is observed that this incomplete configuration of the Circle can be overcome by collateral circulation under auto-regulation mechanism.

3.6 Missing ACoA

Much like the PCoA, the ACoA also plays an important role in collateral circulation under abnormal conditions. The effect of missing ACoA on the cerebral auto-regulation was simulated as shown in Fig. 15. For this configuration, the connecting channel between the left and right ACA is completely disappeared by eliminating the ACoA segment. This case has a relatively large initial drop of 15 percent in mass flux through the left ACA as shown in Fig. 15 (a), while small initial drops of less than 6 percent for the previous cases. Since blood cannot flow to the left ACA through the ACoA, the distal left ACA receives blood only from the bifurcated A1 segments of the left ACA. The flow through the right PCoA changes its direction from the right A1 segment down to the right PCA as arrowed in Fig. 15 (b). The flux through the left PCoA is most increased to deliver more blood to the left MCA as well as the bifurcated A1 segments of the left ACA. Figure 16 shows that both mass fluxes in the left MCA and ACA fail to regain their initial flow rates even after 10 seconds. They have already reached maximum vaso-dilation and thus recovered only about 92 percent of the initial value. This case is physiologically critical where ischemic damages occur to the brain tissues on the front and left sides. It is evident that those communicating arteries (i.e., ACoA and PCoA) are crucial to the normal functioning of the Circle of Willis under auto-regulation mechanism.

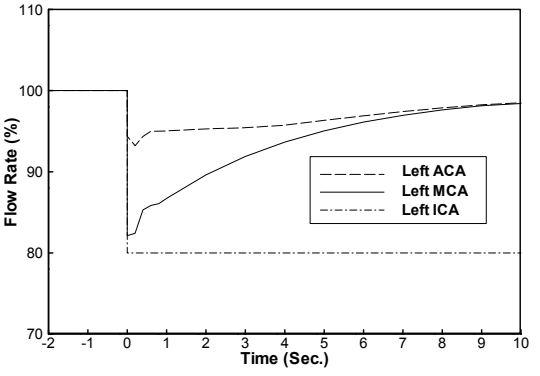

Fig. 14. Percent changes of flow rate in case of missing the left PCoA.

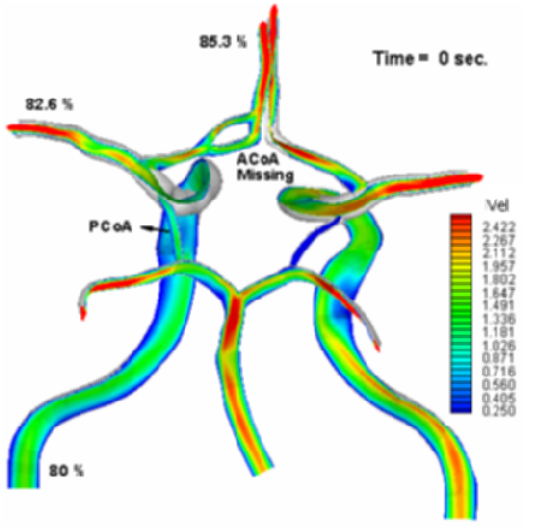

(a) Initial flow distribution: Time = 0 sec

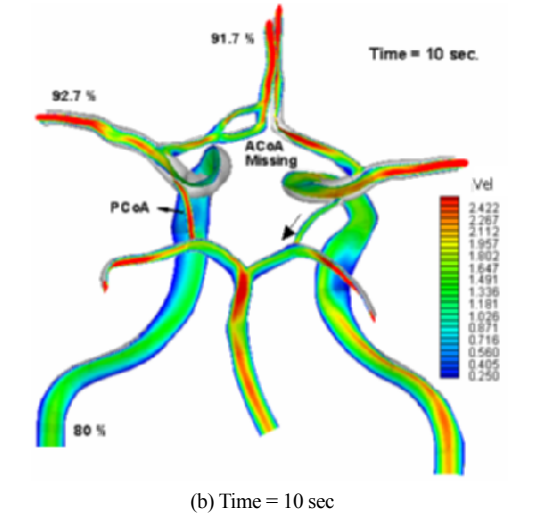

(b) Time = 10 sec

Fig. 15. Flow redistribution in case of missing the ACoA.

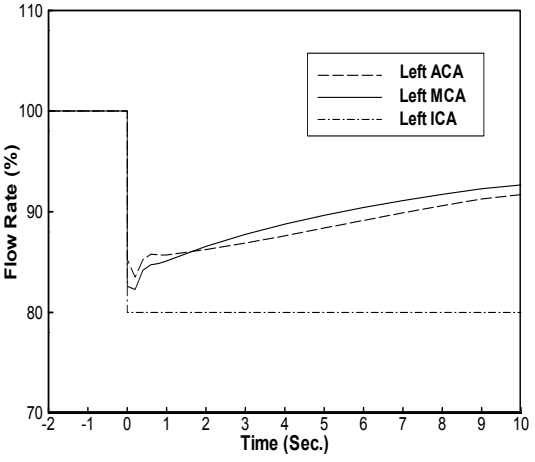

Fig. 16. Percent changes of flow rate in case of missing the ACoA.

4. Conclusion

Numerical simulations using computational fluid dynamics (CFD) have been performed to demonstrate the auto-regulation mechanism and local blood flow in the human brain. A three-dimensional Circle of Willis geometry was reconstructed from the subject-specific magnetic resonance images (MRI) using an image segmentation method and grid generation techniques. The arteriolar auto-regulation algorithm based on a vascular bed model was presented to simulate the self-regulating redistribution of blood flow in the Circle of Willis as well as to impose multiple outflow boundary conditions. These numerical models were applied to a prototype model of the Circle of Willis in order to obtain a preliminary understanding of collateral circulation under auto-regulation. In addition, self-regulating flows through the anatomical Circle of Willis model with various geometrical variants were simulated to investigate the effect of geometrical abnormalities on the redistribution of blood flow in the Circle of Willis. Assuming the left ICA moderately stenosed, abnormal cases of no auto-regulation, missing left PCoA, and missing ACoA were simulated and compared with the original configuration case. It was found that the communicating arteries such as PCoA and ACoA play an important role in proper functioning of cerebral auto-regulation mechanism. The present numerical models combining CFD and MRI are considered to provide the patient-specific information for surgical and interventional procedures as a predictive surgery tool.

Acknowledgements

The author would like to thank Professor Tim David at University of Canterbury for the MRA data sets, and Dr. Dochan Kwak at NASA Ames Research Center and Professor Dongho Lee at Seoul National University for their sincere hospitality. This paper was presented at the Spring Conference to celebrate the 60th anniversary of KSME, and awarded Best Technical Paper at the Fall Conference, 2005. The author also appreciate it.

References

Alpers, B. J., Berry, R. G., Paddison, R. M., 1959, "Anatomical Studies of the Circle of Willis in Normal Brain," *Arch. Neurol. Psychiatry*, Vol. 81, pp. 409~418.

Cebral, J. R., Lohner, R., Burgess, J., 2000, "Computer Simulation of Cerebral Artery Clipping: Relevance to Aneurysm Neuro-Surgery Planning," Proc. ECCOMAS, Sep. 11-14, Barcelona-Spain.

Ferrandez, A., David, T., Brown, M. D., 2002, "Numerical Models of Auto-Regulation and Blood Flow in the Cerebral Circulation," *Computer Methods in Biomechanics and Biomedical Engineering*, Vol. 5 (1), pp. 7~20.

Ferrandez, A., David, T., 2000, "Computational Models of Blood Flow in the Circle of Willis," *Computer Methods in Biomechanics and Biomedical Engineering*, Vol. 4, No. 1, pp. 1~26.

Formaggia, L., Gerbeau, J. F., Nobile., F., Quarteroni, A., 2002, "Numerical Treatment of Defective Boundary Conditions for the Navier-Stokes Equations," *SIAM J. Numer. Anal*. Vol. 40, No. 1, pp. 376~401.

Gijsen, F. J. H., van de Vosse, F. N., Janssen, J. D., 1999, "The Influence of Non-Newtonian Properties of Blood on the Flow in Large Arteries: Steady Flow in a Carotid Bifurcation Model," *Journal of Biomechanics*, Vol. 32, pp. 601~608.

Gray, H., 2000, "Anatomy of the Human Body," 20th Edition by Lewis, W.H., Philadelphia: Lea & Febiger, 1918, New York: Bartleby.com.

Hillen, B., Drinkenburg, B. A., Hoogstraten, H. W., Post, L., 1988, "Analysis of Flow and Vascular Resistance in a Model of the Circle of Willis," *Journal of Biomechanics*, Vol. 21, pp. 807~814.

Kim C. S., "Sensitivity Analysis for the Navier-Stroke Equations with Two-Equation Turbulence Models and Its Applications," Ph.D. Dissertation, Seoul National University, Feb. 2001.

Kim, C. S., Kiris, C., Kwak, D., David, T., 2006,

"Numerical Simulation of Local Blood Flow in the Carotid and Cerebral Arteries Under Altered Gravity," *ASME Journal of Biomechanical Engineering*, Vol. 128, pp.194~202.

Kiris, C., Kwak, D., Rogers, S., Chang, I.-D., 1997, "Computational Approach for Probing the Flow Through Artificial Heart Devices," *ASME Journal of Biomechanical Engineering*, Vol. 119, pp. 452~460.

Kufahl, R. H., Clark, M. E., 1985, "A circle of Willis simulation using distensible vessels and pulsatile flow,", *ASME Journal of Biomechanical Engineering*, Vol. 107, pp. 112~122, 1985.

Kwak, D., Kiris, C., Kim, C. S., 2005, "Aspects Computational Challenges of Viscous Incompressible Flows," *Computers & Fluids*, Vol. 34, pp. 283~299.

Nichols, W. W., O'Rourke, M. F., 1998, "McDonald's Blood Flow in Arteries: Theoretical, Experimental and Clinical Principles," 4th Edition, Arnold, London.

Olufsen, M. S., Nadim, A., Lipsitz, L. A., 2002, "Dynamics of Cerebral Blood Flow Regulation Explained using a Lumped Parameter Model," *Am. J. Physiol.-Regul. Integr*. Comp. Physiol., Vol. 282, R611~R622.

Quarteroni, A., Tuveri, M., Veneziani, A., 2000, "Computational Vascular Fluid Dynamics: Problems, Models and Methods," *Computing and Visualization in Science*, Vol. 2, No.4, pp. 163~197.

Rogers, S. E., Kwak, D., Kiris, C., 1991, "Steady and Unsteady Solutions of the Incompressible Navier-Stokes Equations," *AIAA Journal*, Vol. 29, No. 4, pp. 603~610.

Steinman, D. A., Thomas, J. B., Ladak, H. M., Milnor, J. S., Rutt, B. K., Spence, J. D., 2002, "Reconstruction of Carotid Bifurcation Hemodynamics and Wall Thickness Using Computational Fluid Dynamics and MRI," *Magnetic Resonance in Medicine*, Vol. 47, No. 1, pp. 149~159.

Taylor, C. A., Draney, M. T., Ku, J. P., Parker, D., Steele, B. N., Wang, K., Zarins, C. K., 1999, "Predictive Medicine: Computational Techniques in Therapeutic Decision-Making," *Computer Aided Sur-gery*, Vol. 4, No. 5, pp. 231~247.

Zhao, S. Z., Ariff, B., Long, Q., Hughes, A. D., Thom, S. A., Stanton, A. V., Xu, X. Y., 2002, "Inter-individual Variations in Wall Shear Stress and Mechanical Stress Distributions at the Carotid Artery Bifurcation of Healthy Humans," *Journal of Biome-chanics*, Vol. 35, pp. 1367~1377.